Silicon (2023) 15:3897–3908
https://doi.org/10.1007/s12633-023-02306-9

ORIGINAL PAPER

Effect of Al_3Ni and SiC on Mechanical and Wear Behaviour of Al-Ni-SiC Composite

Manik Mahali[1] · Nitesh Kumar Sinha[1] · I. N. Choudhary[1] · J. K. Singh[1] · S. Mohan[1]

Received: 27 November 2022 / Accepted: 19 January 2023 / Published online: 27 January 2023

Abstract
The present article discusses the combined effect of SiC reinforcement particle and in-situ formed Al_3Ni on the mechanical and wear behavior of Al-Ni-SiC composite. The composite was subjected to examination through microstructure, mechanical and wear properties. The dry sliding pin-on-disc tribometer was utilized to study the wear behaviour of composite at a varying load of 10–20 N and velocities of 1—1.5 m/s with 1500 m sliding distance. Microstructure reveals the formation of in-situ Al_3Ni phase and homogeneous distribution of SiC throughout the matrix. At the same time, it was also indicated that the presence of Al_3Ni phase i.e., hard particle and SiC reinforcement improved the mechanical and wear properties of Al-Ni-SiC composite. The compressive strength and hardness of the composite increase consistently as the reinforcement particle increases. The composite having 16 wt.% SiC shows the high compressive strength and hardness of 732.48 MPa, 49 HV respectively. Composite having 4 wt.% SiC at high load 20 N with each frequency indicates the high wear rate of the given composite. The result of worn surface analysis may be predicted the nature of wear mechanism either adhesive or abrasive with oxidative in nature. The X-Ray Diffraction (XRD) of wear debris also confirms the oxidative nature of wear mechanism.

Keywords Stir casting · Aluminium composite · Microstructure · Wear · Compressive strength

1 Introduction

Aluminium and its alloy are most versatile materials used in different areas viz, aerospace, automobile, marine etc. due to its unique characteristics of having high strength to weight ratio [1–4]. The wide range of Aluminium alloy series has been developed with the variation in the major constituent elements such as manganese, nickel, silicon, copper, magnesium etc. to restrict the suitable application by achieving desired properties [5–10]. The variation in the major constituents may contribute to the evolution of different intermetallic phases Al_2Cu, Al_3Ni, FeAl etc., in the Aluminium alloy which also attribute to the improvement of the mechanical as well as wear properties of an Al-alloy [11–13]. These intermetallics may play a vital role in high temperature application, but somehow the volume fraction of intermetallic can transform ductile to brittle characteristics of an alloy [14].

✉ Manik Mahali
manikmahali.rs.met17@itbhu.ac.in

[1] Metallurgical Engineering Department I.I.T (BHU), Varanasi, Uttar Pradesh 221005, India

Aluminium based metal matrix composite has more attracted toward the automobile and aerospace sectors as compared with Al-alloy. Various researcher fabricated Al-matrix composite having different reinforcement such as Carbide (SiC, TiC, B_4C) [4, 15–17], oxide (Y_2O_3, Al_2O_3) [18–20], Boride (TiB_2) [21, 22], Nitride (AlN, Si_3N_4) [23–26], Hydrates (TiH_2) [27], etc. The reinforced particle having high stiffness and modulus due to which there are high strength and hardness to the matrix [28]. The Properties of composite depends on the wettability of reinforcement, particle size, interface between reinforcement and Al-matrix. The strength of bonding depends upon the thickness of film developed at the interface of matrix and reinforcement particle, which attribute to the load bearing capacity of the composite. Among the various reinforced particle, SiC having high potential of refractoriness, which make suitable candidate for the application of Al-SiC are favoured to the high temperature, wear resistance of the composite [29–31].

The tribological behaviour of metal matrix composite relies on the reinforcement as well as intermetallic compound. The various intermetallic compounds are conjugated with Al-alloy, the formation of most common intermetallic compound in Al-Ni system are Al_3Ni, Al_3Ni_2, Al_3Ni_5, NiAl,

$AlNi_3$ based on percentage of nickel content in aluminium [32–34], these phases are very hard in nature which also act as a reinforcement particle and enhanced the tribological behaviour. In- situ formed Al_3Ni phase are detrimental to the tribological behaviour of composite due to having sharp edge shape. Various researcher has introduced different reinforce particle TiC, TiB_2, Mg_2Si etc. to enhance the tribological behaviour of Al-Ni composite [35–37]. The effect of Al_3Ni and SiC as a reinforcement particle in Al matrix are not widely investigated.

From the literature it has found that the people are always focus in the development of Metal matrix composite and enhancing its properties. But, after the exploration of Aluminium metal matrix hybrid composites in the field of wear there are still limitations in vast areas of wear studies and optimization of its properties. Therefore, in this investigation focus on the combine effect of SiC and in-situ formed Al_3Ni reinforcement on tribological as well as mechanical properties of Al-Ni-SiC composite, fabricated by stir casting method. The incorporation of silicon carbide favoured to tribological behaviour by the transformation of sharp edge Al_3Ni into a fibrous shape. Stir casting method is use to fabricate ex-situ Al-Ni-SiC composite with the variation in the percentage of Ni (5 wt.%) and SiC (4–16 wt.%). The dispersion of SiC in the Al-Ni matrix performed by thermally coating of Silicon carbide on the Al-Ni alloy. The utility of this composites is basically where the abrasive action takes place between two bodies and makes the relative motion in the field of automobile like cylinder liner, disc, connecting rod etc. The characterization technique such as microstructure, X-ray diffraction (XRD) (Model- Rigaku Miniflex 600), scanning electron microscope, atomic force microscopy was used to investigate the wear mechanism as well as mechanical behaviour of Al-Ni-SiC composite.

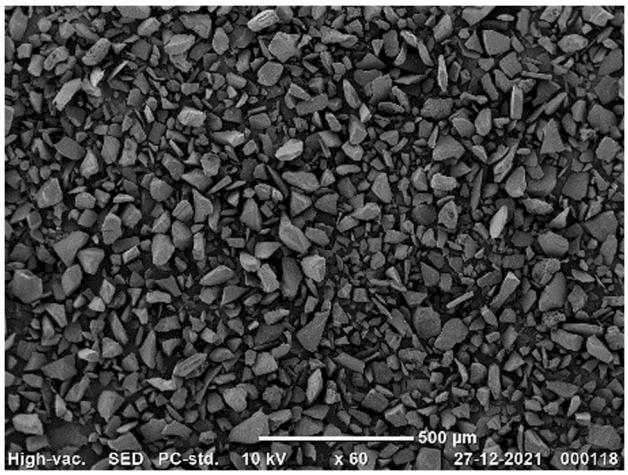

Fig. 1 SEM micrograph of SiC reinforced particle size

2 Materials and Methods

In this investigation Al-Ni master alloy was procured from Matrics Pvt. Lt. (Tamilnadu) (Table 1) and SiC (40–80 micron size) from R.K Scientific (Varanasi). The Scanning electron micrograph (SEM) of reinforcement particle is shown in the Fig. 1.

The effect of SiC on wear properties of Al-Ni-SiC composite with the variation in the load and velocity was investigated. The parameters of wear test are listed in Table 2.

Al-Ni-SiC composite was fabricated using stir casting process as shown in Fig. 2a. Initially Aluminium alloy was melted in a resistance heating furnace at temperature of 720^0C, then pre-heated Al-Ni master alloy was added to achieved Al—5% Ni Alloy. After that pre-heated SiC was added to these melts to achieved Al—5 wt.% Ni-(4 wt.%—16 wt.%) SiC composite and finally poured in copper mold having the dimensions of 10 cm × 5 cm × 5 cm.

A dry sliding pin-on-disc tribometer (Model-Ducom, Serial no-1192) was utilized to analyze the change in wear behavior of Al-Ni-SiC composite. Initially the sample was polished with different grit of emery papers range of 1000–2500 and further clean with acetone before the wear test as shown in Fig. 2b. Ducom tribometer having EN31 disc hardness 65 HRC was used to perform the wear test. The parameter of the wear test was load and velocity, load varies from 10–20 N whereas, velocity varies from 1–1.5 m/s respectively with fixing the sliding distance of 1500 m for all the experiments. These parameters were used to perform the wear test of each sample at ambient temperature as shown in Fig. 2c. The weight loss was calculated on the basic of volume loss that was measured before and after the test. After the test, wear tracks of

Table 1 Chemical composition of the Al-Ni alloy

Composition	Al	Ni	Fe	Cu
Al-5Ni	94.50	5.0	0.001	0.32

Table 2 Wear test parameter

Material	Composite wt.% SiC	Wear testing parameter		
		Load (N)	Velocity (m/sec)	Sliding distance (m)
Al-5 wt.% Ni	Al-5Ni-4SiC	10	1	1500
	Al-5Ni-8SiC	15	2	
	Al-5Ni-12SiC	20		
	Al-5Ni-16SiC			

Fig. 2 **a** Cast product of Al-Ni-SiC composite, **b** wear sample before test **c** wear sample after test

all the sample were examined by the Scanning electron microscope (SEM Model- EVO MA15 / 18) and for surface roughness value the atomic force microscopy (AFM) (Model – NTEGRA Prima) was used.

For Microstructural analysis a conventional route was followed such as grinding and polishing in a different grit of emery paper and then final polishing was done in cloth polisher using alumina suspension. For clear visibility of the phases and particles present in the sample, all the samples were etched with keller's reagent (H_2O-95%, HNO_3-2.5%, HF- 1%, HCl -1.5%) and micrograph of composite was taken using optical microscope (Leica -DFC295). Vickers hardness (model- Leco 700) was used to analyze the microhardness of the composite with 1 kg load and 10 s dwell time. Three different location of the sample was taken the hardness and average values was reported.

The cylindrical shape sample was prepared for compressive test having (diameter 5 mm, height 15 mm). Compressive test was carried out in Instron UTM Machine (Model-Instron 4206) having static load at a fixed strain rate of (10^{-3} s^{-1}) at ambient temperature. Test was done 3 consecutive times and sum of value was reported.

3 Results and Discussion

3.1 XRD

The phase present in the Al-Ni-SiC composite was identified by X-ray diffractometer which is shown in Fig. 3. The phases were identified as α-Al, Ni, SiC, Al_3Ni and Al_3Ni_2. It was observed that with the variation from 4–16 wt.% in SiC there was no extra peak was observed which states that with the addition of SiC, the phase transformations do not take place as which states that SiC in the matrix behaves as an ex-situ reinforced particle. As the Aluminium is matrix materials the Al peaks appeared as sharp and strong.

3.2 Microstructure

Microstructure of Al-Ni-SiC composite with the variation of SiC content are shown in the Fig. 4a–d. The micrograph having α-Al (white), α-Al + Al_3Ni eutectic (bright-dark gray region), SiC (dark polyhedral), Al_3Ni (needle shape) and Al_3Ni_2 are shown in the Fig. 4. The formation of Al_3Ni and Al_3Ni_2 basically depends on the variation of Ni content but the Ni content was 5 percent, the Al_3Ni_2 was embedded inside the Al_3Ni in low magnification it was difficult

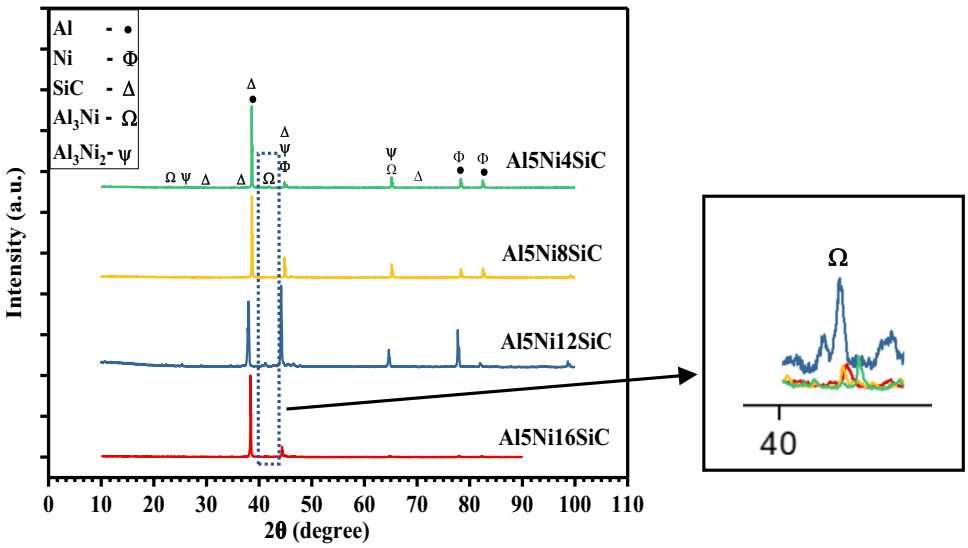

Fig. 3 XRD pattern of Al-Ni-SiC Composite

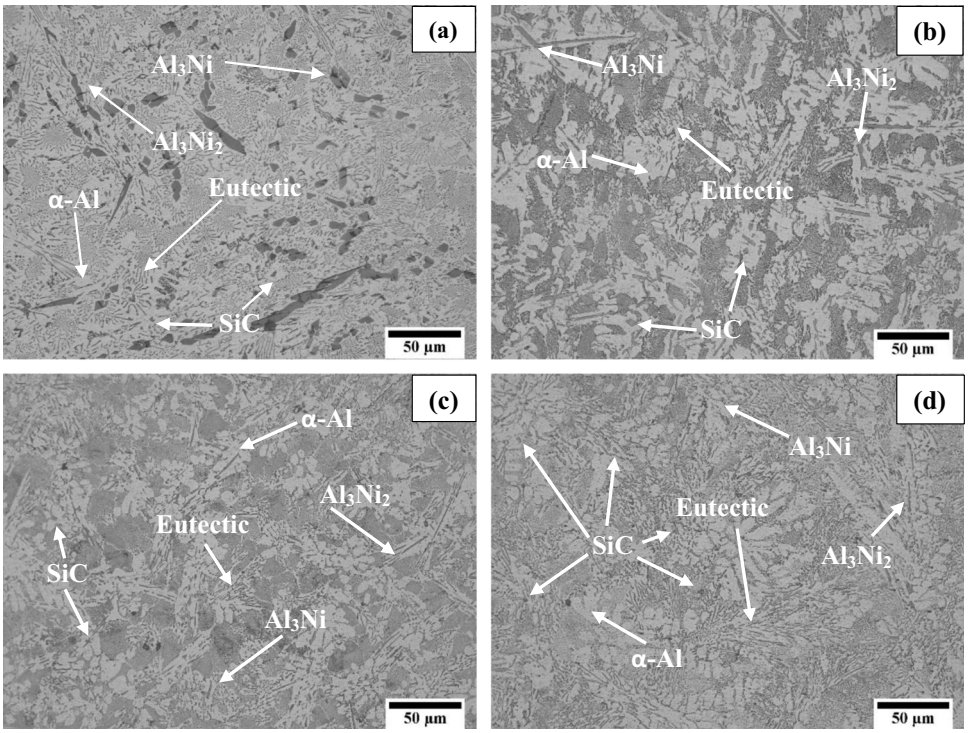

Fig. 4 Optical micrograph of Al-Ni-SiC composite having Al—5 wt.% Ni and **a** 4 wt.% SiC, **b** 8 wt.% SiC, **c** 12 wt.% SiC, **d** 16 wt.% SiC

to distinguished [38]. The Al_3Ni and Al_3Ni_2 are hard phase present in the Al-Ni matrix attribute to a reinforcement in the matrix. The SiC and Al_3Ni are reinforcement particle present in the matrix and uniformly distributed throughout the matrix. SiC help to disintegrate of Al_3Ni and Al_3Ni_2 as shown in the micrograph, as the weight percent of SiC increases from 4 to 16 wt.% which fragments the sharp edge nature of Al_3Ni. Initially the shape of Al_3Ni and Al_3Ni_2 is sharp edge needle structure as shown in Fig. 4a and b, with further addition in SiC the structure of Al_3Ni and Al_3Ni_2 modified to the fibrous form as indicated in Fig. 4c and d. The formation of fibrous Al_3Ni and Al_3Ni_2 enhanced the mechanical properties with variation in the SiC content. The presence of needle shape may attribute to the stress concertation that act as origin of crack initiation which is not desired for material properties.

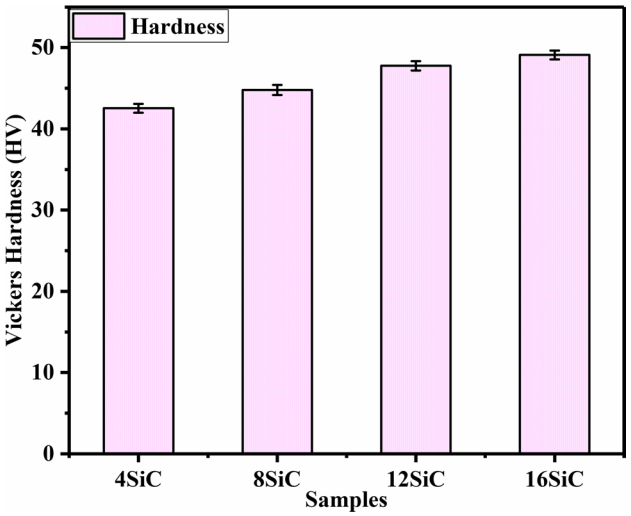

Fig. 5 Vickers's Hardness of the Al-Ni-SiC composite

3.3 Hardness

Vickers's Hardness values of the Al-Ni-SiC composite increases on addition of SiC reinforcement particle. As the SiC is hard particle which influence the hardness of the matrix due to its stiffness, the distribution of SiC and in-situ formed Al_3Ni as well as Al_3Ni_2 also plays a major role to the enhancement of hardness of the matrix. Al_3Ni and SiC act as the nucleation site of the matrix solidification that's refine the grains and make a strong bonding with Aluminium matrix. From the Fig. 5 it was seen from the result that the hardness of matrix having 4 wt.% SiC is low as compared to the 8 wt.% SiC in the matrix, so the 4 wt.% SiC distribution in the matrix not enhanced to the certain range of the matrix hardness. Due to having wide distribution of SiC in the matrix as compared to the 12 wt.% SiC and 16 wt.% SiC composites. Hence the concentration and distribution of the SiC and in-situ formed Al_3Ni as well as Al_3Ni_2 directly proportional to the hardness of composite as shown in Fig. 5 having hardness value 42HV, 44HV, 47HV, and 49HV of 4, 8, 12 and 16 wt.% SiC respectively.

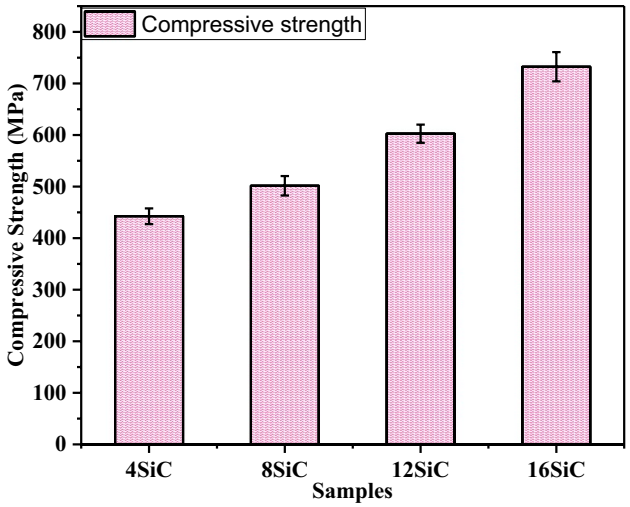

Fig. 6 Compressive strength of Al-Ni-SiC composite

3.4 Compressive Strength

Figure 6 illustrates that the compressive strength of the composite having composition Al 5 wt.% Ni and (4–16) wt.% of SiC. The test was conducted at fixed strain rate of 10^{-3} s^{-1}. The strain that sustains during the test was measured as the total strain of the material was reported in the Table 3. As we increase the SiC percentage the compressive strength also increases consistently. The composite having 16 wt.% SiC shows the higher compressive strength around 732.48 MPa. Result obtained during the test was similar to the conventional strain hardening effect of typical metallic material. The lower value of compressive strength was observed at 4wt%SiC due to having needle shape of Al_3Ni as well as Al_3Ni_2, which forced the shear deformation along shear plane at 45^0 to the loading action. As the percentage of SiC increase, the fibrous Al_3Ni and Al_3Ni_2 resist the shear deformation that results in the weak barreling effect of the matrix and enhanced the compressive strength of composite [39].

3.5 Dry Sliding Pin-on-disc Tribometer

A dry sliding pin-on-disc tribometer was utilized to conduct wear test and compute the wear rate of the Al-Ni-SiC composite by the following Eq. (1). Based on the weight loss with applied load the rate of wear of the composite was estimated as shown in Table 4. The results obtained from wear test were good agreement with the Archard's law that volume of wear debris formed directly related to the applied load and sliding distance.

Table 3 Theoretical calculated strain energy and total strain on static load compressive test

Samples	Strain rate (s^{-1})	Compressive Strength (MPa)	Total Strain (%)	Strain Energy (MJ/m^3)
Al-5Ni-4SiC	10^{-3}	442.46	59.34	147
Al-5Ni-8SiC		501.64	60.76	99
Al-5Ni-12SiC		602.57	66.37	98
Al-5Ni-16SiC		732.48	70.15	169

Table 4 Wear rate of the composite

Sample		Weight loss (gm) 1 m/s	Wear rate (gm/m)	Weight loss (gm) 1.5 m/s	Wear rate (gm/m)
Al5Ni4SiC	10 N	0.0033	2.2×10^{-6}	0.0081	5.4×10^{-7}
	15 N	0.0037	2.4×10^{-6}	0.0083	5.5×10^{-7}
	20 N	0.0062	4.1×10^{-06}	0.00147	9.8×10^{-6}
Al5Ni8SiC	10 N	0.0024	1.6×10^{-6}	0.0054	3.6×10^{-6}
	15 N	0.0037	2.4×10^{-6}	0.0079	5.2×10^{-6}
	20 N	0.0055	3.6×10^{-6}	0.0133	8.8×10^{-6}
Al5Ni12SiC	10 N	0.0022	1.4×10^{-6}	0.0037	2.4×10^{-6}
	15 N	0.003	2×10^{-6}	0.0072	4.8×10^{-6}
	20 N	0.0029	1.9×10^{-6}	0.0107	7.1×10^{-7}
Al5Ni16SiC	10 N	0.0016	1.0×10^{-6}	0.0002	1.4×10^{-6}
	15 N	0.0029	1.9×10^{-6}	0.0052	3.4×10^{-6}
	20 N	0.0029	1.9×10^{-6}	0.0055	4.6×10^{-6}

$$Wear\ rate = \frac{Weight\ loss}{sliding\ distance} \quad (1)$$

3.5.1 Effect of Load

There are various parameters like load, velocity, sliding distance etc. that effects the rate of wear of the material. Figure 7 indicates the weight loss of composite in the variation of load with respect to the sliding velocity and observed that the weight loss of composite was the function of load with respect to velocity. From the Fig. 7a at velocity 1 m/s observed that weight loss increases as the load increases whereas there was decrement in weight loss with respects to the percentage of SiC reinforcement particle. The higher weight loss was observed in the composite having 4 wt.% SiC than the composite having 16 wt.% SiC. It was also indicated that enhanced the wear resistance of the Al-Ni-SiC composite as the SiC content increases similar result was found by Sarmah et.al [37].

The composite having 4—8 wt.% SiC, the nature of weight loss graph was quite similar with the applied load, the weight loss of the composite increase with respect to load. Whereas as the weight % of SiC increase beyond the 8%, the trend of curve was changed. And also observed that composite having 12 wt.% and 16 wt.% have similar nature of curve, which states that as the percentage of SiC increased that enhanced the wear resistance of composite. Therefore, as the increase in content of SiC beyond an optimum percentage that deviate the increasing tendency of curve to declination in weight loss curve. At low wt.% of SiC, the weight loss increases due to the hard SiC and in-situ formed Al_3Ni as well as Al_3Ni_2 particle may act as three body abrasion wear mode after impingement of SiC particles. The composite having beyond 12 wt.% enhanced the wear resistance due to more refinement of Al_3Ni as well as Al_3Ni_2 phase from needle shape to fibrous form, these fibrous shapes improve the hardness of composite and enhanced the load sharing capacity between matrix and reinforcement particle. The fibrous structure resists the detachment of SiC on the surface, which delay the three-body abrasion action and hence enhanced the wear resistance of composite having 16 wt.% SiC as shown in Fig. 7a. As the velocity increases from 1–1.5 m/s as shown in Fig. 7b, the nature of weight loss curve was similar trend of composite having 4–16 wt.% SiC and indicated that the weight loss of composite increases with increasing load. At 20 N load and 1.5 m/s sliding velocity, the composite having 16 wt.% SiC shows more wear resistance as compared with rest [40].

3.5.2 Effect of Velocity

Velocity is also the one of most important parameters to cause a wear phenomenon of the composite. The Fig. 8a shows the effect of velocity with respects to weight loss at constant load of 10 N. The result shows that, as the velocity increases the weight loss of the composite increases and as the weight % of SiC increases, the nature of curve shows the converging trend towards each other, which states that as the weight % of SiC increases the weight loss decreases with respect to increase in velocity. At high load of 15 N and 20 N with the variation in the velocity at 1 m/s and 1.5 m/s, it was observed that there was wide gap between weight loss curves. It was observed that as the velocity increases from 1–1.5 m/s at 10 N -20 N of 4 wt.% SiC the percentage of weight loss increases 145%, 107% and 137% respectively whereas for 16 wt.% SiC the percentage of weight loss increases 25%, 80% and 89% respectively and observed that as the velocity increases weight loss increases. The increased in the velocity at different load shows less variation in weight loss in composite having 16 wt.% SiC as compared with 4 wt.% SiC. Hence 16 wt.% SiC composite shows higher wear resistance with the variation in the velocity at different load due to the modification of Al_3Ni and Al_3Ni_2 shape from needle to fibrous shape [41].

3.5.3 Effect of Load and Velocity on Coefficient of Friction

The coefficient of friction (COF) directly related to applied load, the percentage distribution of ceramic reinforcement

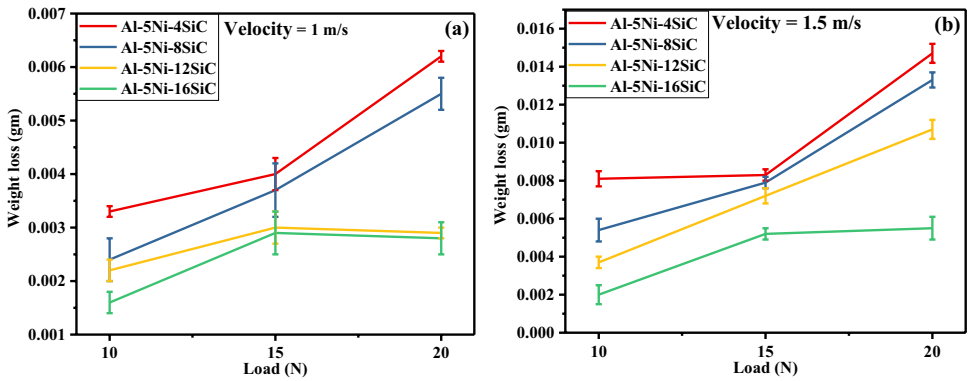

Fig. 7 Weight loss vs Load **a** velocity at 1 m/s **b** velocity at 1.5 m/s

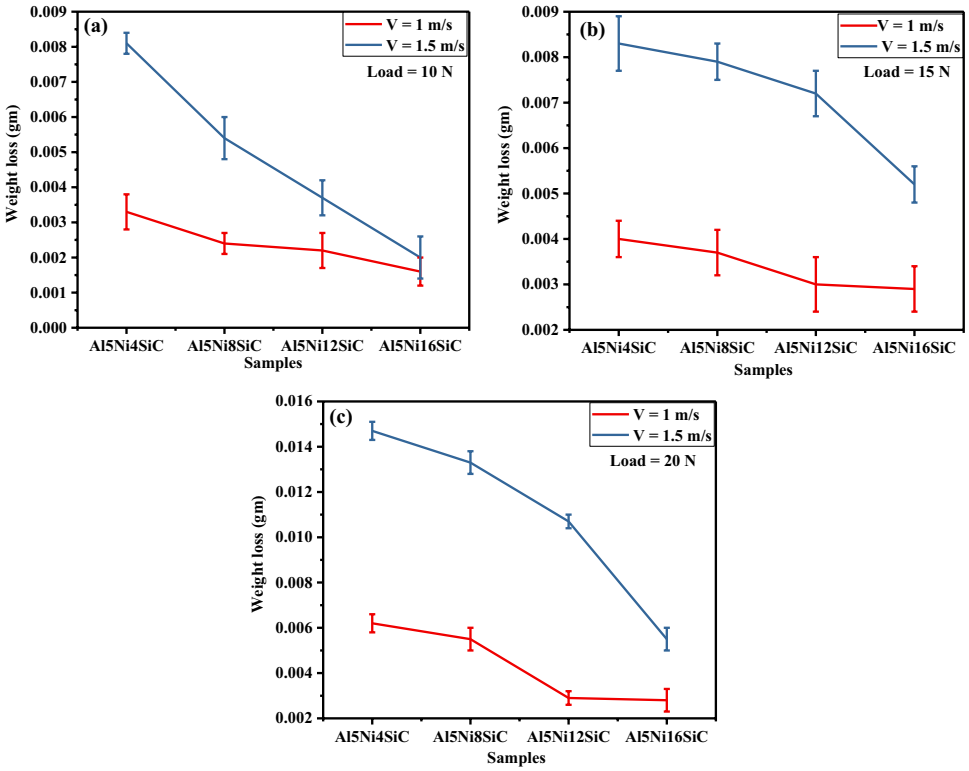

Fig. 8 Effect of velocity and weight loss on Al-Ni-SiC composite at load of **a** 10 N **b** 15 N **c** 20 N

particle SiC, in-situ formed Al_3Ni, Al_3Ni_2 and the velocity employed for the composite sample. It was evident during the performance of wear test that the existence of reinforcement particle in the matrix, applied load and the surface roughness of the sample plays a crucial role to determine coefficient of friction. From the Fig. 9a it was indicated that the COF value varies from 0.1 to 0.9 with the variation of SiC particle. The matrix having 8,12 and 16 wt.% SiC shows the similar range of the COF value during the sliding distance of 1500 m but 4 wt.% SiC has the variation in the COF value during the sliding distance of 1500 m. Up to 750 m travel the COF shows the uniform values of about 0.2 but beyond 750 m it raised in the range of composite having higher percentage of SiC. As the velocity increased to 1.5 m/s it shows similar trends of COF for all the composites. But 4 wt.% SiC has the higher COF in some aspects of distance due to presence of lower amount of SiC particles which at higher velocity shows less wear resistance as compare to other [16].

At load 15 N and velocity 1 m/s, the COF value lies in the range of 0.2 to 0.7 of all the composite but 4 wt.% SiC, 8 wt.% SiC and 16 wt.% SiC shows the COF value in the range of 0.4 to 0.7 in similar fashion but 16 wt.% SiC has the COF value in the range of 0.3 to 0.45 which is lowest among the rest whereas at 12 wt.% of SiC the COF value varies with sliding distance as shown in Fig. 9c, it was observed that up to 1000 m sliding distance the COF value remains constant approximately 0.2 but beyond the 1000 m up to 1500 m of sliding distance, the COF value raised to the range of 0.3 to 0.7. As the velocity increased to 1.5 m/s the COF value ranges from 0.4 to 0.8 which states that as the velocity increase the COF value also increases as shown in Fig. 9d but the composite having 4 wt.% SiC has the higher COF value in the range of 0.6 to 0.8 among the rest, which might be due to having low percentage of SiC reinforcement.

At load of 20 N and velocity 1 m/s the COF value lies in the range from 0.2 to 0.8 of all the composite as shown in Fig. 9e and also observed that the composite having 8 wt.% SiC, 12 wt.% SiC and 16 wt.% SiC shows that the COF values overlap to each other but 4wt%SiC has inhomogeneity in the value of COF as shown in the Fig. 9e, initially 4wt% SiC composite shows the COF value 0.2 up to 300 m of sliding distance beyond 300 m the COF value starts to increase and beyond 600 m the COF value of the composite overlaps with rest. With the increasing velocity from 1 m/s to 1.5 m/s the stacking of COF value was observed as shown in Fig. 9f the composite having low percentage of SiC reinforcement has the higher range of COF and the composite having higher percentage of SiC shows lower COF value [42].

3.5.4 Morphological Analysis of Worn Surface

The worn surface of the composite was investigated by Scanning Electron Microscopy, the morphology of the wear track shows the nature of wear by which it may be predicted about the wear mechanism. The dry sliding wear track of

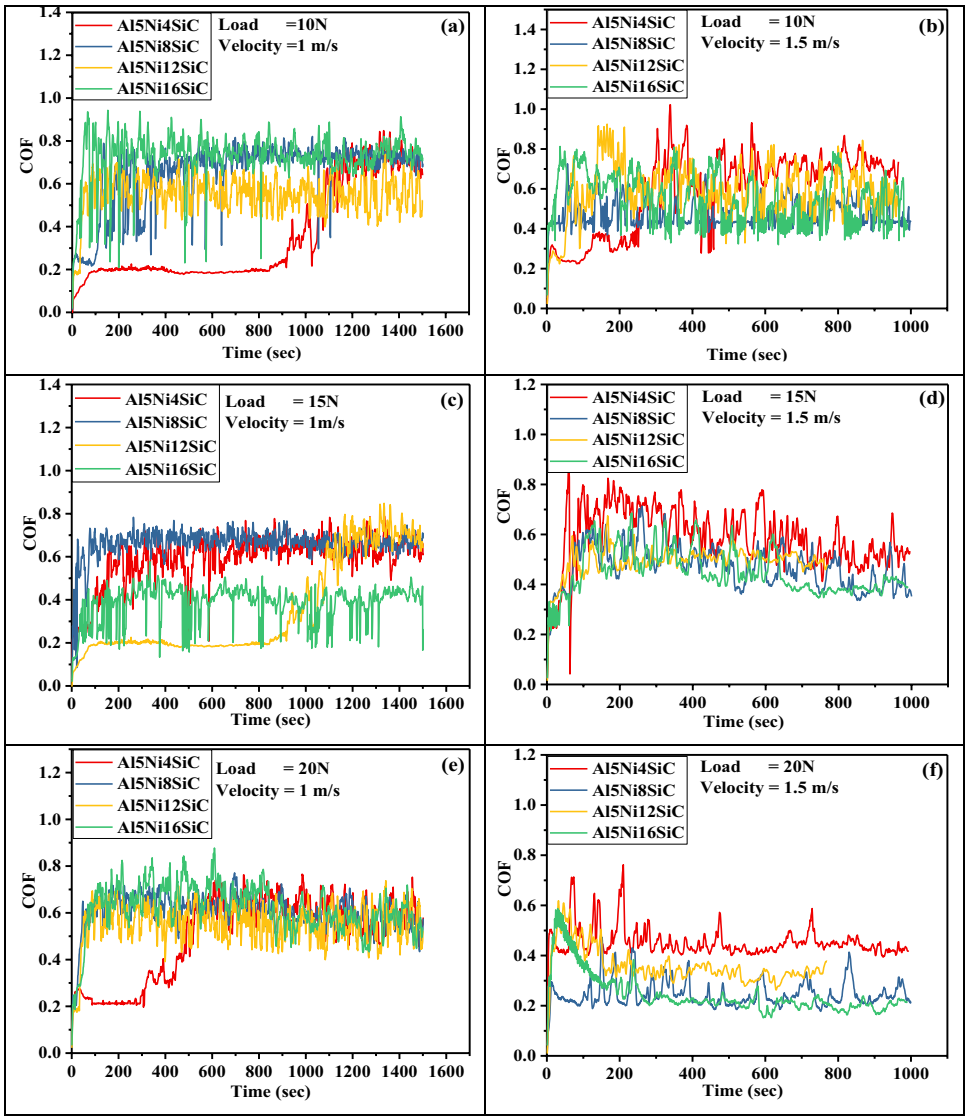

Fig. 9 Coefficient of friction of Al-Ni-SiC composite at velocity 1 m/s and load having **a** 10 N, **c** 15 N, **e** 20 N and at velocity 1.5 m/s having load **b** 10 N, **d** 15 N, and **f** 20 N

the composite are shown in the Fig. 10, signifies the complex phenomena of mixed mode of abrasion and adhesion mechanism. The rubbing action between the sample and disc depends on the sample's surface roughness as well as hardness and applied load which results in the generation of heat, initially at low load (10 N) and low velocity (1 m/s) shallow groves, oxides layer, ploughing surface in some areas having scar mark are shown in Fig. 10a, c, e and g which is due to the abrasion action. As the load (15 N) and velocity (1.5 m/s) increases, the heating action also increase which soften the surface as observed in the Fig. 10d. The heating action facilitates the oxide formation on the surface, which delaminates at higher load (20 N) and velocity (1. 5 m/s) results in the three-body abrasion mechanism and accelerates the wear rate shown in Fig. 10f having marks of deep grooves, oxidative wear etc. The debris particle formed during the sliding of three body abrasive mechanism. This may be due to rubbing of Al_3Ni, Al_3Ni_2 and SiC reinforcement particle in the matrix with hard steel disc [31, 43]. The tribolayer when delaminates the matrix as well as the reinforcement particle to form the finer debris during wear occurs the mechanical alloying. SEM micrograph shows the mechanically mixed layer (MML) formed by the action of force applied which stick to the sample itself [44].

3.5.5 Atomic Force Microscopy Observation

After the dry sliding wear test the surface roughness values and surface morphologies were also the outcomes of the wear behaviour. Characterization of 3D morphology of worn surface was done by atomic force microscopy as indicated in Fig. 11. The sample surface scratches were deeper and wider in case of higher load and higher velocity of 16 wt.% SiC and 12 wt.% SiC containing composite as compare to composite having 8 wt.% SiC and 4 wt.% SiC. The large valleys were in seen composites having 12 wt.% and 16 wt.%

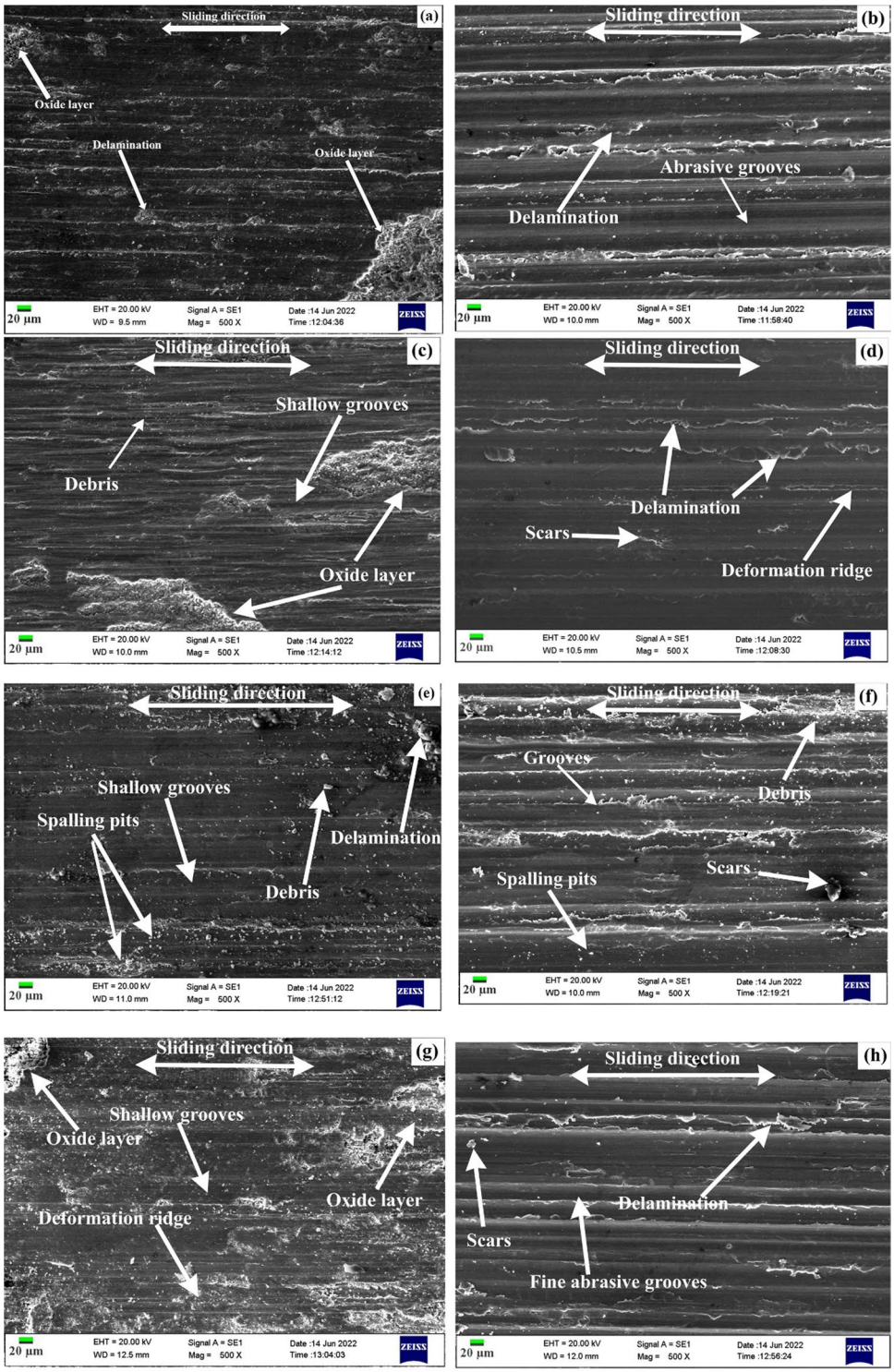

Fig. 10 Surface morphology of wear track at velocity 1 m/s and Load 20 N of Al—5 wt.% Ni **a** 4 wt.% SiC, **b** 8 wt.% SiC, **c** 12 wt.% SiC, **d** 16 wt.% SiC and at velocity 1.5 m/s and Load 20 N **e** 4 wt.% SiC **f** 8 wt.% SiC, **g** 12 wt.% SiC, **h** 16 wt.% SiC

SiC this can be the consequence of sliding after some distance which softened the sample due to rise of temperature during the rubbing of two hard surfaces i.e. composite and steel disc. Those higher concentration and uniformly distributed reinforcement particles created the three-body abrasion situation, which scratches deeper in whole contact areas of the composite sample. These SiC reinforcement particle and Al_3Ni as well as Al_3Ni_2 hard particle give rise to the more surface roughness value. In the AFM Micrograph valleys represents the region of material were removed more as compare to deeper and shallow region. A narrow and shallow valley were seen in composite having 4 wt.% and 8 wt.% of reinforcement particles, in this reason a three-body abrasive effect the less in its action during the wear test [45].

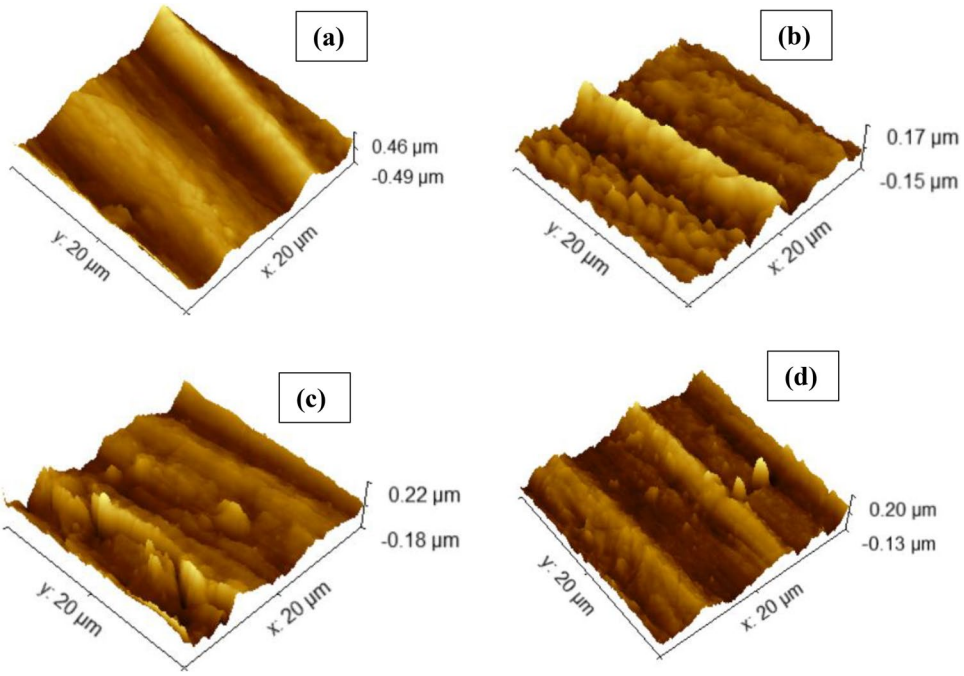

Fig. 11 Surface roughness of composites having **a** 4%SiC, **b** 8%SiC, **c** 12%SiC and **d** 16%SiC at 20 N load and velocity at 1.5 m/s

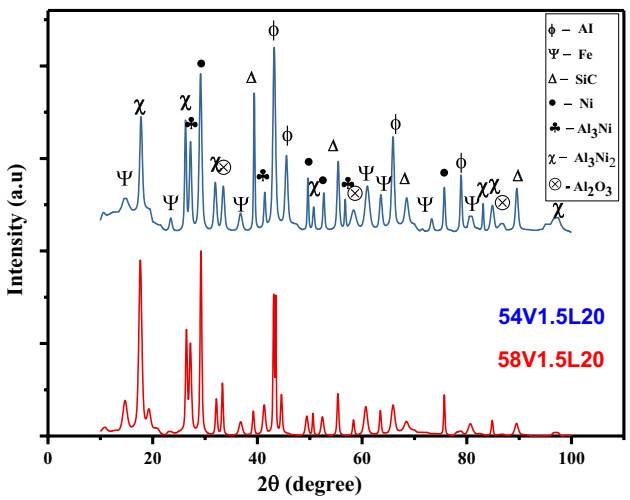

Fig. 12 XRD of Wear debris

3.5.6 XRD of Wear Debris

The X-ray diffraction peak of the wear debris analysis was found to be the presence of phases and formation of compounds in the composite after the wear test. The major phases in the debris are identified as α-Al, SiC, Ni, Fe, Al_3Ni, Al_3Ni_2, Al_2O_3 as shown in Fig. 12. The presence of Iron peak also found in the XRD pattern which depict that the iron particle also impinges from the EN31 disc resulting the abrasive wear between hard particle SiC and Al_3Ni in the composite. Oxidative wear also takes place in the high load (20 N) and high velocity of 1.5 m/s which tells that the oxygen picks up from the atmospheric air because the rise of temperature softens the mechanically mixed tribolayer [46].

4 Conclusion

In the present study, an Al-5Ni-(4–16 wt.%) SiC composite having 5 weight percentage of Nickel and variation of SiC (4–16 wt.%) was successfully fabricated using mechanically stir, casting process. Current findings observed the following conclusion.

1. In fabricated composite the microstructural study revealed that the SiC particle and Al_3Ni phase uniformly distributed throughout the matrix.
2. Compressive strength and hardness of composite having 16 wt.% SiC was increased by 65% and 16% respect to 4 wt. % SiC.
3. It was observed that reinforcement of 16 wt.% SiC particle shows the higher wear resistance of the Al-Ni-SiC composite at higher as well as lower load.
4. Wear test Parameter like load and velocity has the detrimental effect on the tribological behaviour of composite and observed that at low load and low velocity the wear rate was 2.2×10^{-6} whereas at higher load 20 N and 1.5 m/s was 9.8×10^{-6} of composite having 4 wt.% SiC.
5. From the worn morphology of the wear sample, we observed the presence of grooves, scars, deformation ridges, delamination, oxides layer etc. which states that mode of wear mechanism are three body abrasive and adhesive.

6. The XRD of wear debris shows the presence of oxide phase which gives the information of oxidative mode of wear inspite of adhesive and abrasive wear.

Acknowledgements The author sincerely acknowledges the central instrument facility (CIF), IIT (BHU) Varanasi for SEM, XRD, characterisation

Authors Contribution Conceptualization: Manik Mahali; Methodology: Manik Mahali, Nitesh Kumar Sinha; Formal analysis and investigation: Manik Mahali, Ishwari Narain Choudhary; Writing—original draft preparation: Manik Mahali; Writing—review and editing: Manik Mahali, Nitesh Kumar Sinha; Supervision: Prof. Sunil Mohan, Dr. Jayant Kumar Singh.

Data Availability Data and materials supporting the research are found within the manuscript. Raw data files will be provided by the corresponding author upon request.

Declarations

Ethical Approval All author declared that all the ethical standard required for the preparation and publication are complied.

Consent to Participate All person named as author in this manuscript have participated in the planning, design and performance of the research and in the interpretation of the result.

Consent for Publication All authors have indorsed the publication of this research.

Conflict of Interest The authors declare no conflict of interest.

Competing Interests The authors declare no competing interests.

References

1. Cui Y, Wang L, Ren J (2008) Multi-functional SiC/Al composites for aerospace applications. Chinese J Aeronaut 21(6):578–584. https://doi.org/10.1016/S1000-9361(08)60177-6
2. Hernandez FCR, Ramírez JMH, Mackay R (2017) Al-Si alloys: automotive, aeronautical, and aerospace applications. Al-Si Alloy. Automotive, Aeronaut. Aerosp. Appl., pp 1–237. https://doi.org/10.1007/978-3-319-58380-8
3. Wahid MA, Siddiquee AN, Khan ZA (2020) Aluminum alloys in marine construction: characteristics, application, and problems from a fabrication viewpoint. Mar Syst Ocean Technol 15(1):70–80. https://doi.org/10.1007/s40868-019-00069-w
4. Mazaheri Y, Meratian M, Emadi R, Najarian AR (2013) Comparison of microstructural and mechanical properties of Al-TiC, Al-B 4C and Al-TiC-B 4C composites prepared by casting techniques. Mater Sci Eng A 560:278–287. https://doi.org/10.1016/j.msea.2012.09.068
5. Narain V, Ray S (2019) Variation in mechanical properties with MnO2 content in cast and forged in-situ Al-8Mg-MnO2 composites. J Mater Res Technol 8(5):4489–4497. https://doi.org/10.1016/j.jmrt.2019.07.062
6. Rödler G et al (2021) Additive manufacturing of high-strength eutectic aluminium-nickel alloys – Processing and mechanical properties. J Mater Process Technol 298(August):117315. https://doi.org/10.1016/j.jmatprotec.2021.117315
7. Sun S, Hu Q, Lu W, Ding Z, Xia M, Li J (2018) In situ observation on bubble behavior of solidifying Al-Ni alloy under the interference of intermetallic compounds. Metall Mater Trans A Phys Metall Mater Sci 49(10):4429–4434. https://doi.org/10.1007/s11661-018-4818-6
8. Ejiofor JU, Reddy RG (1997) Developments in the processing and properties of particulate Al-Si composites. Jom 49(11):31–37. https://doi.org/10.1007/s11837-997-0008-5
9. Eizadjou M, KazemiTalachi A, DaneshManesh H, Shakur Shahabi H, Janghorban K (2008) Investigation of structure and mechanical properties of multi-layered Al/Cu composite produced by accumulative roll bonding (ARB) process. Compos Sci Technol 68(9):2003–2009. https://doi.org/10.1016/j.compscitech.2008.02.029
10 Valdez S, Campillo B, Pérez R, Martínez L, García HA (2008) Synthesis and microstructural characterization of Al-Mg alloy-SiC particle composite. Mater Lett 62(17–18):2623–2625. https://doi.org/10.1016/j.matlet.2008.01.002
11. Kim K, Kim D, Park K, Cho M, Cho S, Kwon H (2019) Effect of intermetallic compounds on the thermal and mechanical properties of Al-Cu composite materials fabricated by spark plasma sintering. Materials (Basel) 12(9):1–13. https://doi.org/10.3390/ma12091546
12. Kah P, Vimalraj C, Martikainen J, Suoranta R (2015) Factors influencing Al-Cu weld properties by intermetallic compound formation. Int J Mech Mater Eng 10(1). https://doi.org/10.1186/s40712-015-0037-8
13. Ebhota WS, Jen T, Ebhota WS, Jen T. Intermetallics formation and their effect on mechanical properties of and alloys intermetallics formation their effect on mechanical properties of Al-Si-X alloys. https://doi.org/10.5772/intechopen.73188
14. Baker I, George EP (2001) Intermetallics: Nickel Aluminides. Encycl. Mater. Sci. Technol., pp 4225–4231. https://doi.org/10.1016/b0-08-043152-6/00741-5
15. Kumar Show B, Kumar Mondal D, Biswas K, Maity J (2013) Development of a novel 6351 Al-(Al4SiC4+SiC) hybrid composite with enhanced mechanical properties. Mater Sci Eng A 579:136–149. https://doi.org/10.1016/j.msea.2013.04.105
16. Téllez-Villaseñor MA, León-Patiño CA, Aguilar-Reyes EA, Bedolla-Jacuinde A (2020) Effect of load and sliding velocity on the wear behaviour of infiltrated TiC/Cu–Ni composites. Wear 484–485(November):2021. https://doi.org/10.1016/j.wear.2021.203667
17. Samer N et al (2015) Composites : Part A Microstructure and mechanical properties of an Al – TiC metal matrix composite obtained by reactive synthesis. Compos Part A 72:50–57. https://doi.org/10.1016/j.compositesa.2015.02.001
18. Ahamed H, Senthilkumar V (2011) Consolidation behavior of mechanically alloyed aluminum based nanocomposites reinforced with nanoscale Y2O3/Al 2O3 particles. Mater Charact 62(12):1235–1249. https://doi.org/10.1016/j.matchar.2011.10.011
19. Chou S, Huang J, Lii D, Lu H (2007) The mechanical properties and microstructure of Al 2 O 3 / aluminum alloy composites fabricated by squeeze casting. J Alloys Compd 436:124–130. https://doi.org/10.1016/j.jallcom.2006.07.062
20. Bhoi NK, Singh H, Pratap S, Jain PK (2022) Aluminum yttrium oxide metal matrix composite synthesized by microwave hybrid sintering: processing, microstructure and mechanical response. J Inorg Organomet Polym Mater 32(4):1319–1333. https://doi.org/10.1007/s10904-021-02195-8
21 Kennedy AR, Karantzalis AE, Wyatt SM (1999) The microstructure and mechanical properties of TiC and TiB 2 -reinforced cast metal matrix composites. J Mater Sci 34:933–940
22. Branch Z (2013) Fabrication of Al-based composites reinforced with al 2 o 3 -tib 2 ceramic composite particulates using

vortex-casting method. J Mining Metall B 49(3):299–305. https://doi.org/10.2298/JMMB120701032R
23. Pradeepkumar J, Robinson Smart DS, John Alexis S (2018) An aluminium hybrid metal matrix composite reinforced with TaC, Ti, Si3 N4 nanoparticles-A review. Int J Mech Prod Eng Res Dev 2018(Special Issue):187–194
24. Ma X et al (2016) A novel Al matrix composite reinforced by nano-AlN p network. Sci Rep 6:1–8. https://doi.org/10.1038/srep34919
25. Arya RK, Telang A (2020) Silicon nitride as a reinforcement for aluminium metal matrix composites to enhance microstructural, mechanical and tribological behavior. Int J Eng Adv Technol 9(3):3366–3374. https://doi.org/10.35940/ijeat.c6032.029320
26. Sharma P, Sharma S, Khanduja D (2015) Production and some properties of Si 3 N 4 reinforced aluminium alloy composites. J Asian Ceram Soc 3(3):352–359. https://doi.org/10.1016/j.jascer.2015.07.002
27. Rajak DK, Kumaraswamidhas LA, Das S (2016) Investigation and characterisation of aluminium alloy foams with TiH2 as a foaming agent. Mater Sci Technol (United Kingdom) 32(13):1338–1345. https://doi.org/10.1080/02670836.2015.1123846
28. Petrovic JJ, Milewski JV, Rohr DL, Gac FD (1985) Tensile mechanical properties of SiC whiskers. J Mater Sci 20(4):1167–1177. https://doi.org/10.1007/BF01026310
29. Laden K, Guérin JD, Watremez M, Bricout JP (2000) Frictional characteristics of Al-SiC composite brake discs. Tribol Lett 8(4):237–247. https://doi.org/10.1023/A:1019159923619
30. Huang PC, Hou KH, Hong JJ, Lin MH, Wang GL (2021) Study of fabrication and wear properties of Ni–SiC composite coatings on A356 aluminum alloy. Wear 477(January):203772. https://doi.org/10.1016/j.wear.2021.203772
31. Prasad SV, Asthana R (2004) Aluminum metal-matrix composites for automotive applications: tribological considerations. Tribol Lett 17(3):445–453. https://doi.org/10.1023/B:TRIL.0000044492.91991.f3
32. Du Y, Clavaguera N (1996) Thermodynamic assessment of the Al-Ni system. J Alloys Compd 237(1–2):20–32. https://doi.org/10.1016/0925-8388(95)02085-3
33. Li M, Li C, Wang F, Zhang W (2006) Thermodynamic assessment of the Ga-Pt system. Intermetallics 14(7):826–831. https://doi.org/10.1016/j.intermet.2005.12.002
34. Ke L, Huang C, Xing L, Huang K (2010) Al-Ni intermetallic composites produced in situ by friction stir processing. J Alloys Compd 503(2):494–499. https://doi.org/10.1016/j.jallcom.2010.05.040
35. Kumar A, Das AK, Rai PK (2022) Tribological behaviour of Al–Ni–TiB2 composite coating on AA1100 Al-alloy prepared using TIG torch welding route. Trans Indian Inst Met 75(7):1899–1907. https://doi.org/10.1007/s12666-021-02509-x
36 Jin Y, Fang H, Wang S, Chen R, Su Y, Guo J (2022) Effects of Eu modification and heat treatment on microstructure and mechanical properties of hypereutectic Al–Mg2Si composites. Mater Sci Eng A 831(October 2021):142227. https://doi.org/10.1016/j.msea.2021.142227
37. Sarmah P, Patowari PK (2022) Mechanical and tribological analysis of the fabricated Al 6063-based MMCs with SiC reinforcement particles. Silicon (0123456789). https://doi.org/10.1007/s12633-022-02175-8
38. Kundin J, Chen HL, Siquieri R, Emmerich H, Schmid-Fetzer R (2011) Investigation of the heterogeneous nucleation in a peritectic ALNi alloy. Eur Phys J Plus 126(10):1–18. https://doi.org/10.1140/epjp/i2011-11096-6
39. Lee H, Choi JH, Jo MC, Jo I, Lee SK, Lee S (2018) Effects of strain rate on compressive properties in bimodal 7075 Al–SiCp composite. Met Mater Int 24(4):894–903. https://doi.org/10.1007/s12540-018-0092-9
40. León-Patiño CA, Braulio-Sánchez M, Aguilar-Reyes EA, Bedolla-Becerril E, Bedolla-Jacuinde A (2019) Dry sliding wear behavior of infiltrated particulate reinforced Ni/TiC composites. Wear 426–427(January):989–995. https://doi.org/10.1016/j.wear.2019.01.074
41. Vivekananda AS, Prabu SB (2018) Wear behaviour of In Situ Al/TiB2 composite: influence of the microstructural instability. Tribol Lett 66(1):1–14. https://doi.org/10.1007/s11249-018-0990-5
42. Shinde DM, Sahoo P (2022) Influence of speed and sliding distance on the tribological performance of submicron particulate reinforced Al-12Si /1.5 Wt% B4C composite. Int J Met 16(2):739–758. https://doi.org/10.1007/s40962-021-00636-1
43. Sam M, Radhika N (2021) Comparative study on reciprocal tribology performance of mono-hybrid ceramic reinforced Al-9Si-3Cu graded composites. Silicon 13(8):2671–2687. https://doi.org/10.1007/s12633-020-00623-x
44. Li Z, Gao T, Xu Q, Yang H, Han M, Liu X (2019) Microstructure and mechanical properties of an AlN/Mg–Al composite synthesized by Al–AlN master alloy. Int J Met 13(2):384–391. https://doi.org/10.1007/s40962-018-0261-0
45. Yan X, Hu J, Zhang X, Xu W (2022) Tribology international obtaining superior low-temperature wear resistance in Q & P-processed medium Mn steel with a low initial hardness. Tribol Int 175(4):107803
46. Panthglin C, Boontein S, Kajornchaiyakul J, Limmaneevichitr C (2021) The effects of Zr addition on the microstructure and mechanical properties of A356–SiC composites. Int J Met 15(1):169–181. https://doi.org/10.1007/s40962-020-00439-w